Relic Abundance of Asymmetric Dark Matter

Hoernisa Iminniyaz[a*], **Manuel Drees**[b†]   and
Xuelei Chen[c‡]

[a]*School of Physics Science and Technology, Xinjiang University,*
Urumqi 830046, China
[b]*Bethe Center for Theoretical Physics and Physikalisches Institut, Universität Bonn,*
Nussallee 12, 53115 Bonn, Germany
[c]*National Astronomical Observatories, Chinese Academy of Sciences,*
Beijing 100012, China

Abstract

We investigate the relic abundance of asymmetric Dark Matter particles that were in thermal equilibrium in the early universe. The standard analytic calculation of the symmetric Dark Matter is generalized to the asymmetric case. We calculate the asymmetry required to explain the observed Dark Matter relic abundance as a function of the annihilation cross section. We show that introducing an asymmetry always reduces the indirect detection signal from WIMP annihilation, although it has a larger annihilation cross section than symmetric Dark Matter. This opens new possibilities for the construction of realistic models of MeV Dark Matter.

[*]wrns@xju.edu.cn

[†]drees@th.physik.uni-bonn.de

[‡]xuelei@cosmology.bao.ac.cn

1   Introduction

One of the most striking features of cosmology today is that the Universe contains a large amount of Dark Matter, whose mass density exceeds that of the known baryonic matter by about five times. Cosmic microwave background (CMB) anisotropy observations by the Wilkinson Microwave Anisotropy Probe (WMAP) yield an accurate determination of the total amount of the Dark Matter [1],

$$\Omega_{\mathrm{DM}} h^2 = 0.1109 \pm 0.0056 \,, \tag{1}$$

where Ω_{DM} is the Dark Matter (DM) density in units of the critical density, and $h = 0.710 \pm 0.025$ is the Hubble constant in units of $100 \ \mathrm{km} \ \mathrm{sec}^{-1} \ \mathrm{Mpc}^{-1}$.

Although we already have a relatively precise measurement of the Dark Matter density, we still do not know what the Dark Matter is. Neutral, long–lived or stable weakly interacting massive particles (WIMPs) are currently considered as excellent candidates for Dark Matter. One of the most popular WIMP Dark Matter candidate is the neutralino in supersymmetric theory, which is stable due to the conserved R–parity [2]. Neutralinos are Majorana particles, i.e. they are their own anti–particles. However, this is only one possibility and we do not actually have any evidence that the Dark Matter consists of Majorana particles. Indeed, most of the known elementary particles are not Majorana particles, but rather have distinct anti–particles; moreover, the ordinary matter in the Universe is almost entirely made from baryons, with anti–baryons contributing only a tiny fraction of the baryons. It is thus natural to consider asymmetric Dark Matter (ADM), for which particles and anti–particles are not identical. This allows scenarios where the universe exhibits a Dark Matter asymmetry, i.e. there are more Dark Matter particles than anti–particles (or vice versa).

One motivation for considering this scenario is that the average density of baryons is comparable to that of Dark Matter; with $\Omega_b \approx 0.046$, they differ only by a factor of about five. This led to speculations that a common mechanism might give rise to the known baryon asymmetry and a postulated asymmetry in the Dark Matter sector [3, 4].

One attractive feature of the WIMP Dark Matter scenario is that it provides a natural explanation for the observed Dark Matter abundance (the "WIMP miracle"). At early time when the interaction rates are high, the WIMP particles are in thermal equilibrium with the rest of the cosmic fluid. As the Universe expands and the temperature of the fluid drops, the interaction rates become smaller. Eventually the Dark Matter particles decouple from the rest of the cosmic fluid, so that their co–moving density is constant ("frozen"). For symmetric Dark Matter, the resulting relic abundance is of the same order of magnitude as the observed value, if the WIMP annihilation cross section is of weak size. This hints at a connection between weak–scale physics (which is also being probed at colliders) and Dark Matter.

The abundance of Dark Matter can be calculated by solving the Boltzmann equation which describes the time evolution of particle densities in the expanding Universe. In case of symmetric Dark Matter, such calculations have been done for various standard [5, 6] and nonstandard [7, 8] cosmological scenarios.

In this work we generalize this calculation to the case of asymmetric Dark Matter. We solve the relevant Boltzmann equations both numerically and in an analytic approximation. We assume that WIMPs can annihilate only with their anti–particles, so that the number of particles minus the number of anti–particles in a co–moving volume is conserved. Without loss of generality we assume that there are more particles than anti–particles.[*] We assume that the Dark Matter asymmetry, if any, is created well before Dark Matter annihilation reactions freeze out. Moreover, we assume standard cosmology during and after WIMP decoupling. This implies a constant co–moving entropy density, and absence of late non–thermal WIMP production (e.g. from the decay of heavier particles).

This paper is arranged as follows. In Sec. 2, we discuss the Boltzmann equations and the relic abundance of asymmetric Dark Matter. In Sec. 3, we derive an approximate analytical formula for the asymmetric case. In general the resulting Dark Matter density depends both on the Dark Matter asymmetry and on the Dark Matter annihilation cross section. In Sec. 4, we obtain constraints on these parameters from the observed Dark Matter relic abundance. We also compute the ratio of anti–particle and particle densities in the allowed part of parameter space, and show that a non–vanishing asymmetry leads to a reduced rate of WIMP annihilation in galactic haloes. Finally, in Sec. 5 we summarize our results and draw some conclusions.

2 Relic Abundance of Asymmetric Dark Matter

Consider a Dark Matter particle denoted by χ that is *not* self–conjugate, i.e. the anti–particle $\bar{\chi} \neq \chi$. The relic densities of χ and $\bar{\chi}$ are determined by solving the Boltzmann equations which describe the time evolution of the number densities n_χ, $n_{\bar{\chi}}$ in the expanding universe. Under the assumptions that only $\chi\bar{\chi}$ pairs can annihilate into Standard Model (SM) particles, while $\chi\chi$ and $\bar{\chi}\bar{\chi}$ pairs cannot, the relevant Boltzmann equations are:

$$
\begin{aligned}
\frac{\mathrm{d}n_\chi}{\mathrm{d}t} + 3Hn_\chi &= -\langle\sigma v\rangle(n_\chi n_{\bar{\chi}} - n_{\chi,\mathrm{eq}} n_{\bar{\chi},\mathrm{eq}}) \ ; \\
\frac{\mathrm{d}n_{\bar{\chi}}}{\mathrm{d}t} + 3Hn_{\bar{\chi}} &= -\langle\sigma v\rangle(n_\chi n_{\bar{\chi}} - n_{\chi,\mathrm{eq}} n_{\bar{\chi},\mathrm{eq}}) \ .
\end{aligned}
\tag{2}
$$

During the radiation dominated epoch, the expansion rate is given by

$$
H = \frac{\pi T^2}{M_{\mathrm{Pl}}} \sqrt{\frac{g_*}{90}} \ ,
\tag{3}
$$

---

[*]In other words, we define the "particle" to be the one with the larger density, if an asymmetry exists.

where $M_{\rm Pl} = 2.4 \times 10^{18}$ GeV is the reduced Planck mass, and g_* is the effective number of the relativistic degrees of freedom. Here we will consider only the case of cold Dark Matter, i.e. we assume the Dark Matter particles were already non–relativistic at decoupling. The equilibrium number densities $n_{\chi,\rm eq}$ and $n_{\bar{\chi},\rm eq}$ are then given by

$$
\begin{aligned}
n_{\chi,\rm eq} &= g_\chi \left(\frac{m_\chi T}{2\pi} \right)^{3/2} {\rm e}^{(-m_\chi + \mu_\chi)/T}, \\
n_{\bar{\chi},\rm eq} &= g_\chi \left(\frac{m_\chi T}{2\pi} \right)^{3/2} {\rm e}^{(-m_\chi - \mu_\chi)/T},
\end{aligned}
\tag{4}
$$

where m_χ is the mass of the WIMP, μ_χ is the chemical potential of the particles, and g_χ is the number of the internal degrees of freedom of the χ particle. We have used the fact that $\mu_{\bar{\chi}} = -\mu_\chi$ in equilibrium. As a result, the chemical potential drops out in the product $n_{\chi,\rm eq} n_{\bar{\chi},\rm eq}$. In Eqs.(2) the term proportional to this product describes $\chi\bar{\chi}$ production from SM particles; it is clear that this term should not be affected by the WIMP chemical potential.[†]

We follow the standard picture of the Dark Matter particle evolution. At high temperature the χ and $\bar{\chi}$ particles are in thermal equilibrium in the early universe. When T drops below the mass m_χ, the number densities $n_{\chi,\rm eq}$ and $n_{\bar{\chi},\rm eq}$ decrease exponentially, as long as $m_\chi > |\mu_\chi|$. Eventually the interaction rates $\Gamma = n_{\bar{\chi}} \langle \sigma v \rangle$ and $\bar{\Gamma} = n_\chi \langle \sigma v \rangle$ therefore drop below H, which scales like T^2, see Eq.(3). The χ and $\bar{\chi}$ distributions are then no longer kept in chemical equilibrium, and their co–moving number densities approach constants. The temperature at which the WIMPs drop out of chemical equilibrium is called the freeze–out temperature.

The Boltzmann equations (2) can be rewritten in terms of the dimensionless quantities $Y_\chi = n_\chi/s$, $Y_{\bar{\chi}} = n_{\bar{\chi}}/s$, and $x = m_\chi/T$, where

$$
s = (2\pi^2/45) g_* T^3
\tag{5}
$$

is the entropy density. If we assume that the universe expands adiabatically during this period, the Boltzmann equations become

$$
\frac{dY_\chi}{dx} = -\frac{\lambda \langle \sigma v \rangle}{x^2} \left(Y_\chi Y_{\bar{\chi}} - Y_{\chi,\rm eq} Y_{\bar{\chi},\rm eq} \right);
\tag{6}
$$

$$
\frac{dY_{\bar{\chi}}}{dx} = -\frac{\lambda \langle \sigma v \rangle}{x^2} \left(Y_\chi Y_{\bar{\chi}} - Y_{\chi,\rm eq} Y_{\bar{\chi},\rm eq} \right),
\tag{7}
$$

where we have introduced the constant

$$
\lambda = \frac{4\pi}{\sqrt{90}} m_\chi M_{\rm Pl} \sqrt{g_*}.
\tag{8}
$$

[†]Here we ignore effects due to Bose enhancement or Fermi suppression in the *final* state, as usual in the treatment of the decoupling of WIMPs. These effects become important only if the Dark Matter particles were (semi–)relativistic at decoupling [6].

Subtracting Eq.(6) from Eq.(7), we obtain

$$\frac{dY_\chi}{dx} - \frac{dY_{\bar{\chi}}}{dx} = 0 \,. \tag{9}$$

This implies

$$Y_\chi - Y_{\bar{\chi}} = C \,, \tag{10}$$

where C is a constant, i.e. the difference of the co–moving densities of the particles and anti–particles is conserved. This follows from our assumption that χ and $\bar{\chi}$ only annihilate with each other, which could e.g. be due to conservation of some (global) charge.[‡] Inserting Eq.(10) into Eqs.(6) and (7), our Boltzmann equations become

$$\frac{dY_\chi}{dx} = -\frac{\lambda\langle\sigma v\rangle}{x^2} \left(Y_\chi^2 - CY_\chi - P\right); \tag{11}$$

$$\frac{dY_{\bar{\chi}}}{dx} = -\frac{\lambda\langle\sigma v\rangle}{x^2} \left(Y_{\bar{\chi}}^2 + CY_{\bar{\chi}} - P\right), \tag{12}$$

where

$$P = Y_{\chi,\mathrm{eq}}Y_{\bar{\chi},\mathrm{eq}} = (0.145 g_\chi/g_*)^2 \, x^3 \, \mathrm{e}^{-2x} \,. \tag{13}$$

As noted above, P does not depend on the chemical potential μ_χ, which simplifies our calculation. These equations can be solved numerically; a semi–analytical solution will be presented in the next Section.

In most cases, the WIMP annihilation cross section can be expanded in the relative velocity v between the annihilating WIMPs[§]

$$\sigma v = a + bv^2 + \mathcal{O}(v^4) \,. \tag{14}$$

If $\chi\bar{\chi}$ annihilation from an $S-$wave initial state is unsuppressed, the first term in Eq.(14) dominates, while for annihilation from a $P-$wave initial state, $a = 0$ but in general $b \neq 0$. In all examples we know, annihilation from either the $S-$ or the $P-$wave (or both) is allowed; the expansion (14) is then sufficient for an accuracy of a few percent.

In Fig. 1 we show the evolution of the relic abundances for asymmetric Dark Matter χ and its anti–particle $\bar{\chi}$ as function of $x = m/T$.[¶] Here we take $b = 0$ for simplicity, with $a = 5 \times 10^{-9}\mathrm{GeV}^{-2}$ and $C = 10^{-11}$. Results with non–vanishing b are qualitatively the same. For comparison, we also show result for the symmetric case ($C = 0$). We show the actual as

---

[‡]C is proportional to the initial (high$-T$) value of the $\chi - \bar{\chi}$ asymmetry, $A_\chi = (n_\chi - n_{\bar{\chi}})/(n_\chi + n_{\bar{\chi}})$. However, A_χ will change with time or temperature once the WIMPs become non–relativistic, approaching a (larger) constant again once the WIMPs decouple. We therefore prefer to use C rather than A_χ to parameterize the $\chi - \bar{\chi}$ asymmetry.

[§]See ref.[9] for a discussion of scenarios where this expansion does not work.

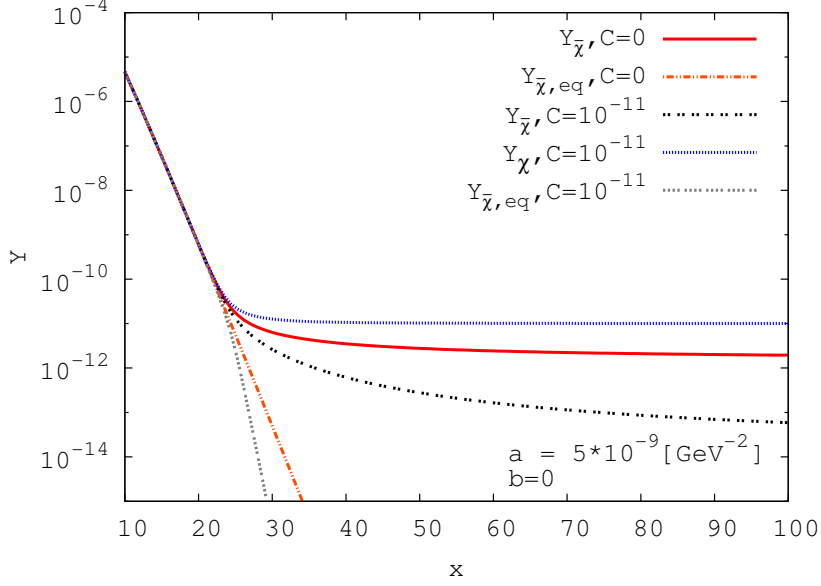[¶]Similar numerical results have been presented in ref, [4],

Figure 1: The evolution of the scaled χ and $\bar{\chi}$ abundances as function of $x = m/T$ for $a = 5 \times 10^{-9}$ GeV^{-2}, $b = 0$, $m = 100$ GeV and $C = 10^{-11}$ or zero. The $\bar{\chi}$ equilibrium distributions are shown for comparison.

well as equilibrium values of the $\bar{\chi}$ density; for $C = 0$ ($C > 0$), the equilibrium χ density is equal to (larger than) the equilibrium $\bar{\chi}$ density shown in the figure. Note that χ and $\bar{\chi}$ are distinct particles even if $C = 0$.

As we can see in the figure, at high temperature (small x) Y_χ and $Y_{\bar{\chi}}$ are very close to their equilibrium values. This is true irrespective of the initial value $Y_\chi(x_0)$ as long as x_0 is somewhat smaller than the freeze–out value x_F, $x_0 - x_F \gtrsim 1$ [8]. Moreover, $Y_{\chi,\text{eq}}(x)$ is almost independent of C as long as $Y_{\chi,\text{eq}}(x; C = 0) > C$. This inequality is satisfied for

$$x < x_C \simeq -\ln(C') + \frac{3}{2}\ln[-\ln(C')], \tag{15}$$

with $C' = 2^{5/2}\pi^{7/2}g_*C/(45g_\chi) \simeq 310C$; in the last step we have taken $g_\chi = 2$, $g_* = 90$. Numerically, $x_C \simeq 24$ for $C = 10^{-11}$. x_C is therefore also close to the value where the $\bar{\chi}$ density begins to differ significantly from its equilibrium value, which signals the on–set of decoupling. For $C = 0$ the actual $\bar{\chi}$ density then rather quickly approaches a constant.

For $C = 10^{-11}$ the $\bar{\chi}$ abundance begins to deviate from its equilibrium value also at $x \approx 23$. However, it keeps decreasing for a large range of x−values, only slowly approaching a smaller constant value ($\sim 10^{-13}$) at very large x. The evolution of the χ abundance is even more remarkable: we have not plotted its equilibrium density in this figure, because for $C = 10^{-11}$ it almost coincides with the actual χ density at all temperatures! The ratio $Y_\chi/Y_{\chi,\text{eq}}$ never exceeds 1.85; this maximum value is reached for $x \simeq 25$. This can be understood from the observation that the χ density becomes nearly equal to its equilibrium value, simply given by

C, also at very large x, where the $\bar{\chi}$ density is very small.

This large difference in the evolution of the χ and $\bar{\chi}$ densities originates again from our assumption that only $\chi\bar{\chi}$ pairs can annihilate. Since Y_χ is bounded from below by C, $\bar{\chi}$ particles still find a significant density of partners for annihilation even after the nominal decoupling temperature. This explains why $Y_{\bar{\chi}}$ keeps decreasing even at rather large x. This in turn means that χ particles find even fewer partners for annihilation than in the symmetric case ($C = 0$). The χ density therefore "decouples" (i.e., $\Gamma_\chi < H$) even earlier than for $C = 0$, although its number density never differs very much from its equilibrium value, as we just saw.
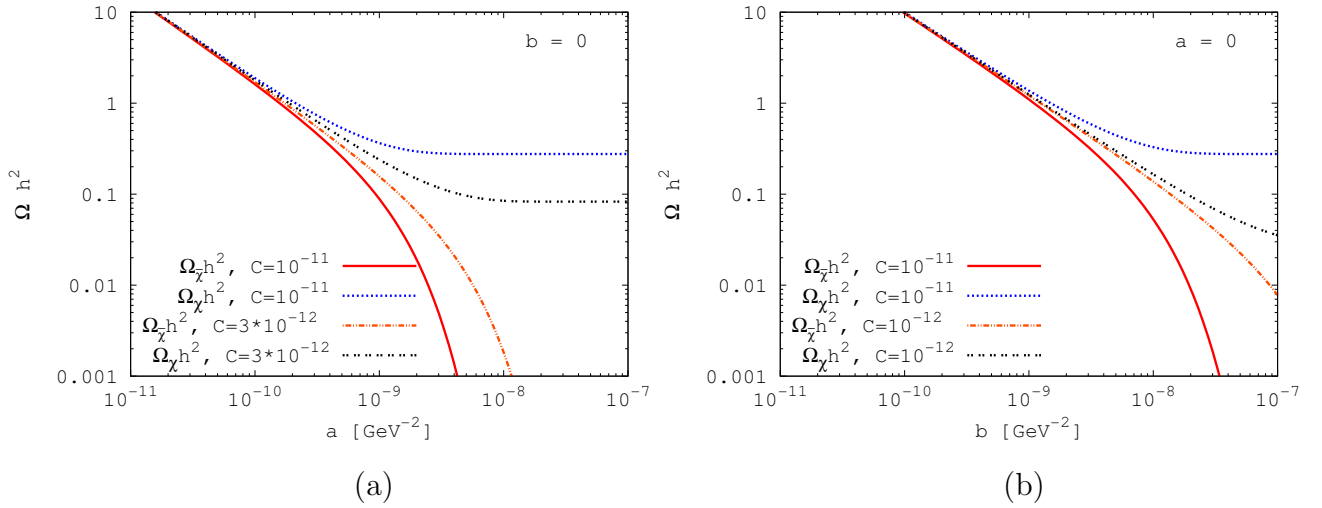

Figure 2: The relic density Ωh^2 for particle χ and anti–particle $\bar{\chi}$ as a function of the cross section. Here we take $m_\chi = 100$ GeV, $g_\chi = 2$ and $g_* = 90$. Panel (a) is for $b = 0$, while panel (b) is for pure $P-$wave annihilation ($a = 0$).

With this understanding of the asymmetric Dark Matter thermal decoupling, we now look at how its abundance depends on the annihilation cross section. In Figure 2(a,b) we plot the relic density Ωh^2 for particle χ and anti–particle $\bar{\chi}$ as a function of the annihilation cross section, with two different values of C. In panel (a) we assume a constant ($S-$wave) cross section ($b = 0$), while panel (b) is for a pure $P-$wave case ($a = 0$).

We see that for small $\chi\bar{\chi}$ annihilation cross section the relic density is independent of the asymmetry. This is the case whenever the relic density in the symmetric case ($C = 0$) is much larger than the assumed value of C; in this situation the small asymmetry clearly does not play much of a role in the decoupling dynamics. Since for $C = 0$ the relic density scales essentially inversely with the annihilation cross section, this scenario corresponds to small cross sections. More precisely, the product of annihilation cross section and asymmetry determines whether the asymmetry has significant impact on the final relic density or not.

In the regime of small cross section the velocity dependence of the cross section is relevant. In the symmetric case the contribution of the $b-$term in Eq.(14) to the final relic density is suppressed by a factor $x_F/3 \simeq 7$ relative to that of the $a-$term. A similar scaling holds in Fig. 2 for small cross section.

On the other hand, as already shown in Fig. 1, for sufficiently large annihilation cross section a non–vanishing asymmetry C does greatly affect the relic density. The scaled χ density Y_χ will then simply approach C, while the final $\bar{\chi}$ density becomes insignificant. This is the limit of extremely asymmetric dark matter. The total DM relic density then becomes independent of the value and the velocity dependence of the cross section (although the velocity dependence does play a role in deciding what cross sections are "large" in this sense).

3 Analytical Solution

While the Boltzmann equations (11), (12) can be solved numerically, it is still useful to have some analytical solution of these equations, as in the symmetric Dark Matter case. In our semi–analytical treatment we closely follow the standard treatment [5] of symmetric Dark Matter to solve Eq.(12) for the $\bar{\chi}$ density. The χ density can then be computed trivially using Eq.(10).

We begin by introducing the quantity $\Delta_{\bar{\chi}} = Y_{\bar{\chi}} - Y_{\bar{\chi},\mathrm{eq}}$. Its evolution follows directly from the Boltzmann equation (12):

$$\frac{d\Delta_{\bar{\chi}}}{dx} = -\frac{dY_{\bar{\chi},\mathrm{eq}}}{dx} - \frac{\lambda \langle \sigma v \rangle}{x^2} \left[\Delta_{\bar{\chi}}(\Delta_{\bar{\chi}} + 2Y_{\bar{\chi},\mathrm{eq}}) + C\Delta_{\bar{\chi}} \right] . \tag{16}$$

We consider the behavior of the solution of this equation in two regimes. At sufficiently high temperature $Y_{\bar{\chi}}$ tracks its equilibrium value $Y_{\bar{\chi},\mathrm{eq}}$ very closely. In that regime $\Delta_{\bar{\chi}}$ is small, and $d\Delta_{\bar{\chi}}/dx$ and $\Delta_{\bar{\chi}}^2$ are negligible. The Boltzmann equation (16) then becomes

$$\frac{dY_{\bar{\chi},\mathrm{eq}}}{dx} = -\frac{\lambda \langle \sigma v \rangle}{x^2} \left(2\Delta_{\bar{\chi}} Y_{\bar{\chi},\mathrm{eq}} + C\Delta_{\bar{\chi}} \right) . \tag{17}$$

In order to calculate the left–hand side of Eq.(17), we need an explicit expression for the equilibrium density $Y_{\bar{\chi},\mathrm{eq}}(x)$. By definition the right–hand sides of the Boltzmann equations (6) and (7) vanish in equilibrium. Hence the right–hand side of Eq.(12) should vanish as well for $Y_{\bar{\chi}} = Y_{\bar{\chi},\mathrm{eq}}$, which implies

$$Y_{\bar{\chi},\mathrm{eq}}^2 + CY_{\bar{\chi},\mathrm{eq}} - P = 0 . \tag{18}$$

This quadratic equation has two solutions, but only one of them yields a positive $\bar{\chi}$ equilibrium density:

$$Y_{\bar{\chi},\mathrm{eq}} = -\frac{C}{2} + \sqrt{\frac{C^2}{4} + P} . \tag{19}$$

Plugging Eq.(19) into Eq.(17) and ignoring x relative to x^2, we have

$$\Delta_{\bar{\chi}} \simeq \frac{2x^2 P}{\lambda \langle \sigma v \rangle (C^2 + 4P)}. \tag{20}$$

This solution will be used to determine the freeze–out temperature for $\bar{\chi}$, which we denote by $\bar{x}_F$.

At sufficiently low temperature, i.e. for $x > \bar{x}_F$, we can ignore the production term $\propto Y_{\bar{\chi},\mathrm{eq}}$ in the Boltzmann equation (16), so that

$$\frac{d\Delta_{\bar{\chi}}}{dx} = -\frac{\lambda \langle \sigma v \rangle}{x^2} \left(\Delta_{\bar{\chi}}^2 + C\Delta_{\bar{\chi}} \right). \tag{21}$$

At this point we may assume $\Delta_{\chi}(\bar{x}_F) \gg \Delta_{\chi}(\infty)$. Integrating Eq.(21) from $\bar{x}_F$ to ∞ then yields

$$Y_{\bar{\chi}}(x \to \infty) = \frac{C}{\exp\left(C\lambda \int_{\bar{x}_F}^{\infty} \langle \sigma v \rangle\, x^{-2} dx \right) - 1}. \tag{22}$$

If we use the non–relativistic expansion (14) of the cross section times relative velocity, the thermal averaging gives

$$\langle \sigma v \rangle = a + 6\, b x^{-1} + \mathcal{O}(x^{-2}). \tag{23}$$

The solution (22) then becomes

$$Y_{\bar{\chi}}(x \to \infty) = \frac{C}{\exp\left[C(4\pi/\sqrt{90})\, m_{\chi} M_{\mathrm{Pl}} \sqrt{g_*}\, (a\, \bar{x}_F^{-1} + 3b\, \bar{x}_F^{-2}) \right] - 1}, \tag{24}$$

where we have used Eq.(8). Note that for small asymmetry C, or more precisely for small argument of the exponential in the denominator, C will drop out, and the $\bar{\chi}$ relic density will be inversely proportional to the annihilation cross section. This reproduces the standard result [5]. On the other hand, Eqs.(22) or (24) indicate that the $\bar{\chi}$ relic density will become exponentially small if the product of annihilation cross section and asymmetry becomes large.

We can repeat this exercise to calculate the relic density of χ particles. The result is

$$Y_{\chi}(x \to \infty) = \frac{C}{1 - \exp\left[-C(4\pi/\sqrt{90})\, m_{\chi} M_{\mathrm{Pl}} \sqrt{g_*}\, (a x_F^{-1} + 3b x_F^{-2}) \right]}, \tag{25}$$

where x_F is the inverse scaled freeze–out temperature of χ. Note that Eqs.(24) and (25) are only consistent with the constraint (10) if $x_F = \bar{x}_F$. Recall from the discussion in the previous Section that for sizable C the reaction rate Γ_{χ} is (much) smaller than the rate $\Gamma_{\bar{\chi}}$, since χ particles find (far) fewer partners for annihilation. The fact that our treatment nevertheless requires equal "freeze–out" temperatures for χ and $\bar{\chi}$ particles indicates that the intuitive condition $\Gamma(x_F) \simeq H(x_F)$, i.e. reaction rate $\simeq$ expansion rate, can no longer be applied consistently for the decoupling of asymmetric Dark Matter.

For convenience, we express the final abundance in terms of

$$\Omega_\chi h^2 = \frac{m_\chi s_0 Y_\chi(x \to \infty) h^2}{\rho_{\text{crit}}} \, , \tag{26}$$

where $s_0 = 2.9 \times 10^3 \text{ cm}^{-3}$ is the present entropy density, and $\rho_{\text{crit}} = 3 M_{\text{Pl}}^2 H_0^2$ is the present critical density. The corresponding prediction for the present relic density for Dark Matter is given by

$$\Omega_{\text{DM}} h^2 = 2.76 \times 10^8 \, m_\chi \left[Y_\chi \left(x \to \infty \right) + Y_{\bar\chi} \left(x \to \infty \right) \right] \text{GeV}^{-1} \, . \tag{27}$$

For small product of annihilation cross section and asymmetry the WIMP mass m_χ drops out in the final result (27). In contrast, if this product becomes large, the $\bar\chi$ relic density is negligible while the scaled χ relic number density is simply given by C; in this limit the final Dark Matter mass density is thus proportional to the mass of the Dark Matter particle. In that regard the Dark Matter mass density of very asymmetric WIMPs behaves like that of hot Dark Matter, although our WIMPs remain cold Dark Matter.

The remaining task is to fix the freeze–out temperature. Here the standard method [5] needs some modification. We start from the standard definition of $\bar x_F$ which assumes that freeze–out occurs when the deviation $\Delta_{\bar\chi}$ is of the same order as the equilibrium value of $Y_{\bar\chi}$:

$$\xi Y_{\bar\chi,\text{eq}}(\bar x_{F_0}) = \Delta_{\bar\chi}(\bar x_{F_0}) \, , \tag{28}$$

where ξ is a numerical constant of order unity. We adopt the usual value [5] $\xi = \sqrt{2} - 1$. By comparing with numerical solutions, we find that the standard treatment under–predicts the $\bar\chi$ relic density for sizable asymmetry. To very good approximation the ratio of the exact analytical solution and the approximation using $\bar x_{F_0}$ as decoupling temperature only depends on the product $\lambda C \langle \sigma v \rangle (x_{F_0})/x_{F_0}^2$, rather than on C, m_χ and the annihilation cross section separately. This is not so surprising, since this expression appears as integrand in Eq.(22). Moreover, the ratio of exact and approximate solution remains of order unity as long as the above product is $\lesssim 1$.

We therefore need only a relatively minor modification of the standard treatment. After some trials, we found that the most elegant and simple way to improve the analytical approximation is through a small shift of the freeze–out temperature:

$$\bar x_F = \bar x_{F_0} \left(1 + \frac{0.285\lambda \, aC}{\bar x_{F_0}^3} + \frac{1.350\lambda \, bC}{\bar x_{F_0}^4} \right) \, . \tag{29}$$

In Fig. 3 we plot the ratio of the exact value of the $\bar\chi$ particle abundance to our analytical approximation. As shown in the figure, the approximate analytic result matches the exact numerical result very well as long as $\lambda C \langle \sigma v \rangle (x_F)/x_F^2 \lesssim 1$. For even larger product of cross section and asymmetry the deviation becomes sizable again. However, in that case the $\bar\chi$
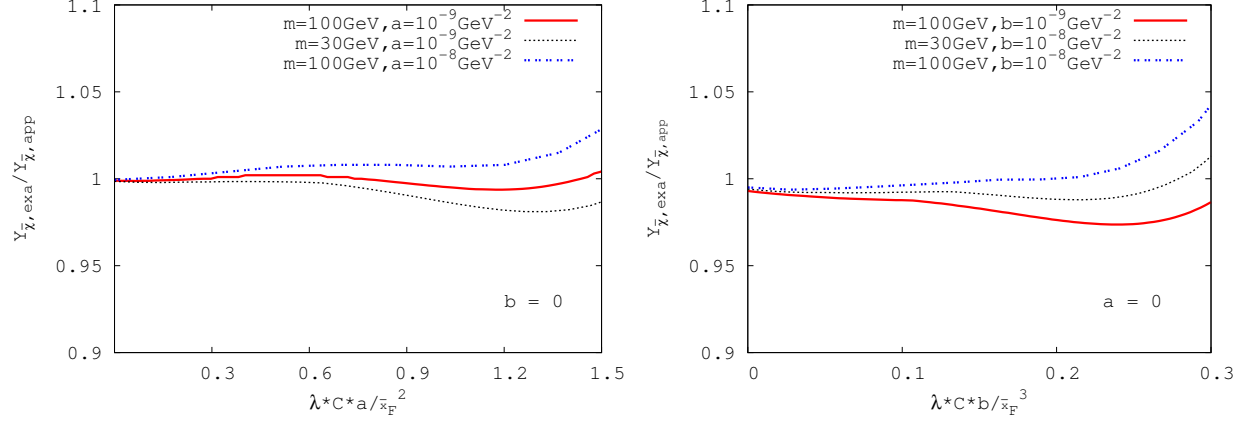
9

Figure 3: The ratio of the exact value of the $\bar{\chi}$ particle abundance to the analytic value of $\bar{\chi}$ particle abundance.

relic density is entirely negligible. Quantitatively, our approximation reproduces the exact numerical solution to better than 2% (5%) as long as the final $\bar{\chi}$ relic density exceeds 10^{-4} (10^{-9}) times the final χ relic density.

Since for large product $\lambda C \langle \sigma v \rangle$ the scaled χ relic number density is simply given by C, our simple approximation reproduces the exact χ relic density, and also the exact total WIMP ($\chi + \bar{\chi}$) mass density, to better than 2% for all combinations of parameters.

We finally note that the shift (29) of $\bar{x}_F$ amounts to $\lesssim 2\%$ for the parameter range covered in Fig. 3. This nevertheless can lead to a significant change of the $\bar{\chi}$ relic density due to the exponential dependence of Eq.(24) on $\bar{x}_F$.

4   Constraints on Parameter Space and Indirect Detection Signals

The Dark Matter abundance can be derived from cosmological observations. This measurement does not depend on the nature of dark matter, e.g. whether it is symmetric or asymmetric, as long as the Dark Matter particles are sufficiently slow ("cold" Dark Matter). Using only the CMB data, the WMAP team derived the Dark Matter density given in Eq.(1) for the minimal ΛCDM model. The precision could be further improved by including observations of baryon acoustic oscillation (BAO) and/or direct measurements of the Hubble constant (H_0) into the fits [1]. We note that besides the statistical error quoted in Eq.(1), there could also be systematic errors, and the result depends somewhat on the model and priors adopted. Nevertheless, we may use the measured Dark Matter abundance to place constraints on the

asymmetric Dark Matter model. In view of the above remarks, we adopt the conservative range

$$0.10 < \Omega_{\mathrm{DM}} h^2 < 0.12 \tag{30}$$

when setting bounds on the model parameters; this is roughly the $\pm 2\sigma$ limit for the abundance indicated by the WMAP fit given in Eq.(1). Note that for asymmetric Dark Matter, the χ and $\bar{\chi}$ contributions have to be added:

$$\Omega_{\mathrm{DM}} = \Omega_\chi + \Omega_{\bar{\chi}} \,. \tag{31}$$

In this Section we assume that the annihilation cross section is given by Eq.(14). We use exact numerical solutions of the Boltzmann equations; however, the analytical solution described in the previous Section reproduces the exact result to better than 5% for all combinations of parameters we analyze in this Section.
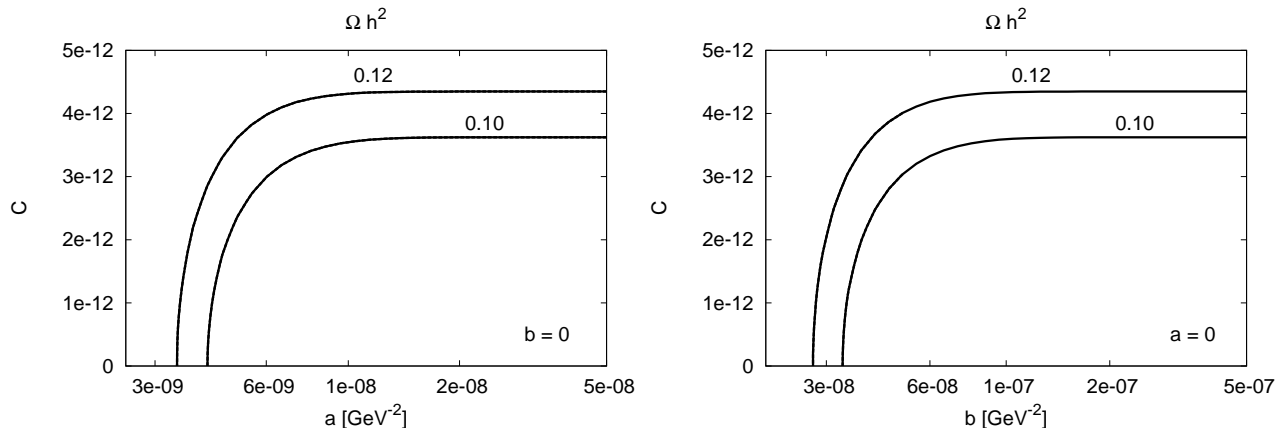

Figure 4: The allowed region in the (a, C) plane for $b = 0$ (left), and in the (b, C) plane for $a = 0$ (right), when the Dark Matter density Ωh^2 lies between 0.10 and 0.12. Here we take $m_\chi = 100$ GeV, $g_\chi = 2$ and $g_* = 90$; the allowed values of C scale to good approximation like $1/m_\chi$.

The relation between the cross section parameters a and b (for $b = 0$ and $a = 0$, respectively) and the asymmetry C are shown in Fig. 4 for two values of the total Dark Matter density. For $C = 0$, i.e. in the symmetric case, one needs $a \sim 4 - 5 \times 10^{-9}$ GeV^{-2} for $b = 0$ (i.e. $S-$wave dominance), and $b \sim 3 \times 10^{-8}$ GeV^{-2} for $a = 0$ ($P-$wave dominance). These cross sections are about two times larger than the cross sections required for self–conjugate (Majorana) Dark Matter with $g_\chi = 2$ degrees of freedom. This is due to the fact that the (equal) χ and $\bar{\chi}$ contributions have to be added, as in Eq.(31); each of them is about as large as the contribution from Majorana dark matter with the same cross section. The resulting doubling of the total Dark Matter density has to be corrected by also (approximately) doubling

the annihilation cross section.*

Now consider the asymmetric case, i.e. $C \neq 0$. For small values of C, the abundance is not much affected, so the iso–abundance contours initially rise almost vertically. This can be understood from the analytical expressions (24) and (25): if we ignore the shift of $\bar{x}_F$ given by (29), which is very small for small C, we find $Y_\chi(x \to \infty) \simeq Y_\chi(x \to \infty; C = 0) + C/2 + \mathcal{O}(C^2)$ and $Y_{\bar{\chi}}(x \to \infty) \simeq Y_\chi(x \to \infty; C = 0) - C/2 + \mathcal{O}(C^2)$, i.e. the correction to the total Dark Matter relic density begins at $\mathcal{O}(C^2)$.

For somewhat larger cross sections the curves quickly flatten out. A larger cross section leads to smaller decoupling temperature, and hence to a smaller relic density; this has to be compensated by increasing C. Specifically, once the cross section is twice as large as that required for vanishing asymmetry, the required asymmetry is already only about 5% smaller than the asymptotic value required for large annihilation cross section (i.e., for strongly asymmetric Dark Matter, where the $\bar{\chi}$ relic density is negligible and the χ density is simply given by C). Since $C = 0$ gives the minimal allowed value of $\langle \sigma v \rangle$ while $\langle \sigma v \rangle \longrightarrow \infty$ defines the maximal allowed value of C, the above statement can be written as

$$C(\langle \sigma v \rangle > 2\langle \sigma v \rangle|_{\text{min}}) > 0.95 C_{\text{max}} . \tag{32}$$

Of greater physical interest than the ratio C/C_{max} are the fraction $Y_{\bar{\chi}}/Y_\chi$ as well as the product $\sigma Y_\chi Y_{\bar{\chi}}$, where the particle densities are to be taken at the present epoch, i.e. for very large x. These quantities are shown in Figs. 5 and 6, respectively.

The ratio $Y_{\bar{\chi}}/Y_\chi$ determines the contribution of anti–particles to the current Dark Matter density. In the left frame of Fig. 5 this ratio is shown as function of $m_\chi \cdot C$, so that the results are nearly independent of m_χ; the annihilation cross section has been chosen such that the relic density has the indicated value ($\Omega_{\text{DM}} h^2 = 0.10$ [0.12] for the black [grey or red] curves). Plotted in this way, the result is almost independent of whether the $a-$ or $b-$term in the annihilation cross section (14) dominates.

We see that for small C the logarithm of the ratio falls essentially linearly with increasing C, with relatively gentle slope. Recall from the discussion of Fig. 4 that for constant annihilation cross section the ratio would behave approximately like $[Y_\chi(C = 0) - C/2]/[Y_\chi(C = 0) + C/2]$ for sufficiently small C; this gives $\ln(Y_{\bar{\chi}}/Y_\chi) \simeq -C/Y_\chi(C = 0)$. Fig. 4 also showed that increasing C requires at first only very small increase of the annihilation cross section.

---

*One can also compare non self–conjugate Dark Matter with Majorana Dark Matter with $g_\chi = 4$. Note that for fixed annihilation cross section, the final relic density depends on g_χ only logarithmically (via x_f). An asymmetric Dark Matter scenario with given cross section then corresponds to a model of Majorana Dark Matter with half the cross section, since in the non self–conjugate case effectively only half the initial states contribute to the annihilation ($\chi\bar{\chi}$ and $\bar{\chi}\chi$ contribute but $\chi\chi$ and $\bar{\chi}\bar{\chi}$ do not).
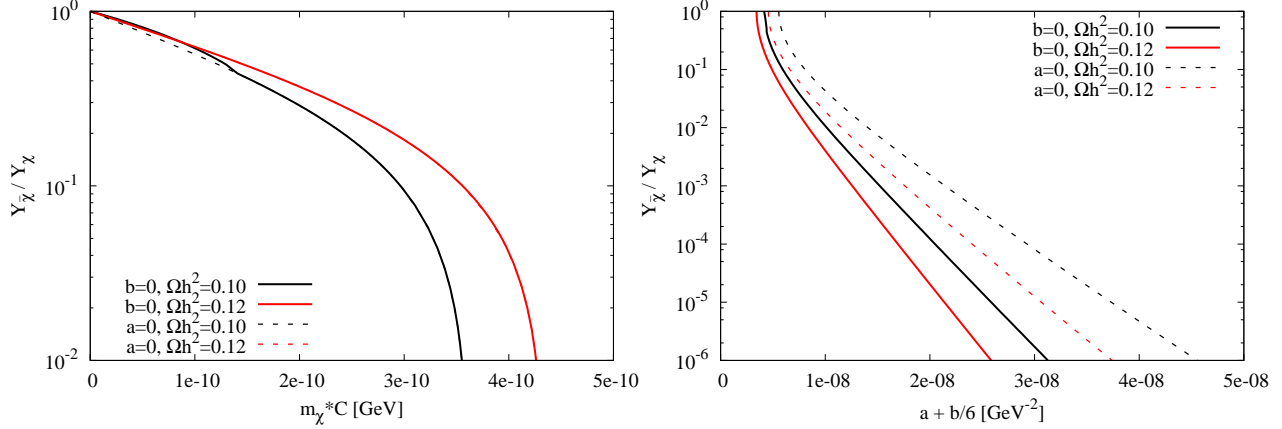
Figure 5: Ratio of the current anti–particle abundance $Y_{\bar{\chi}}$ to the particle abundance Y_χ as a function of $m_\chi \cdot C$ (left) or the sum $a + b/6$ characterizing the annihilation cross section (right) for different combinations of cross sections and total Dark Matter relic density. In the left (right) frame the annihilation cross section (asymmetry C) is chosen such that the total dark matter density $\Omega_{\text{DM}}h^2$ has the indicated value. Results are for $g_* = 90$ and $m_\chi = 100$ GeV, but are almost independent of m_χ.

This behavior continues until C reaches about 95% of its maximal value, where the ratio $Y_{\bar{\chi}}/Y_\chi \simeq 0.03$. When C is increased even more the ratio plummets. This is caused by the required increase of the annihilation cross section, which has to become very large as $C \longrightarrow C_{\max}$. We saw in Fig. 2 that this strongly suppresses the $\bar{\chi}$ relic density. The logarithmic slope of the ratio therefore approaches $-\infty$ as $C \to C_{\max}$.

In this region of large asymmetry it therefore seems more useful to consider the ratio as function of the annihilation cross section. This is shown in the right frame of Fig. 5. We have chosen $a + b/6$ as x–axis, so that the cases $a = 0$ (dashed curves) and $b = 0$ (solid) can be shown on the same scale. The asymmetry C is chosen such that the total relic density has the indicated value. We see that the ratio first decreases very quickly when the annihilation cross section is increased beyond its minimal possible value, which is reached for $C = 0$. This corresponds to the rapid increase of the required asymmetry C with increasing cross section shown in Fig. 4. For cross sections larger than roughly twice the minimal value the curves flatten out, and have essentially constant logarithmic slope from then on; this slope depends on the desired relic density and on the functional form of the cross section (a– or b–dominance).

The product $\sigma Y_\chi Y_{\bar{\chi}}$ determines the strength of indirect Dark Matter detection signals from the annihilation of WIMPs in the haloes of galaxies. In Fig. 6 this product is normalized to the same product taken at $C = 0$, i.e. for symmetric Dark Matter. Notice that the cross section in the normalization factor is kept fixed, to the value required to get the indicated Dark Matter relic density, while the cross section in the numerator is allowed to vary. Gravity acts the same way on particles and anti–particles, and the WIMP distribution in the present
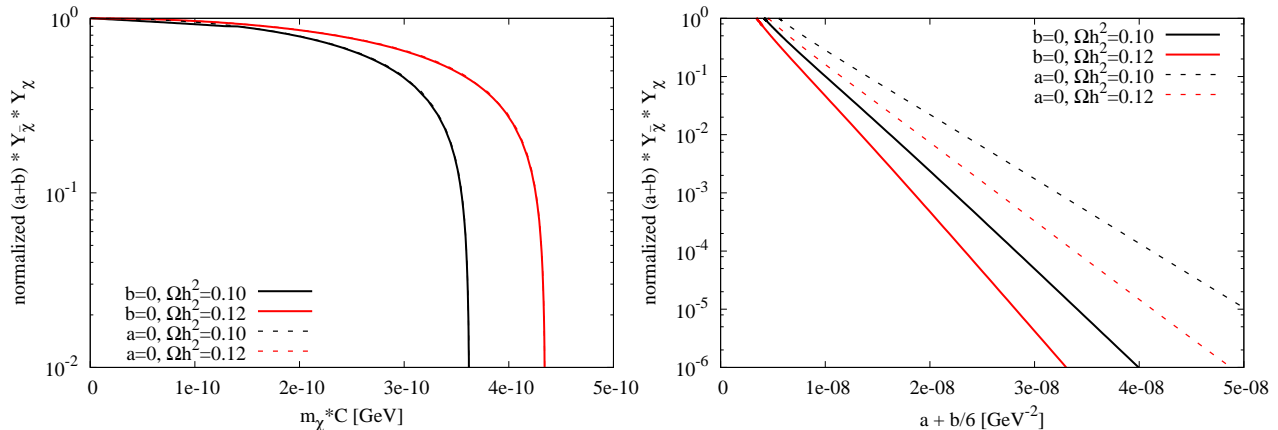
13

Figure 6: Today's annihilation rate for asymmetric Dark Matter divided by the same quantity for symmetric Dark Matter ($C = 0$), as a function of $m_\chi \cdot C$ (left) and $a + b/6$ (right). Parameters and conventions are as in Fig. 5.

universe is basically only determined by gravity.[†] The ratio $n_{\bar\chi}/n_\chi$ should therefore be equal to the universally averaged $Y_{\bar\chi}/Y_\chi$ everywhere. This normalized product thus shows how the strength of indirect Dark Matter detection signals varies over the allowed parameter space.

In the case at hand, even for $C = 0$ particles can only annihilate with anti–particles. For given total Dark Matter density and given annihilation cross section the annihilation rate will therefore be two times smaller than for self–conjugate (Majorana) Dark Matter. This is essentially compensated by the fact that we need approximately two times larger annihilation cross sections for $C = 0$ to achieve a given total Dark Matter density, compared to the case of Majorana dark matter; see the discussion of Fig. 4. Fig. 6 can therefore also be used to compare with the more frequently studied case of Majorana Dark Matter.

The left frame of Fig. 6 shows the normalized product $\sigma \cdot Y_\chi \cdot Y_{\bar\chi}$ as function of $m_\chi \cdot C$, which again makes the result almost independent of m_χ. We also note that, as in the left frame of Fig. 5, the result is almost identical for $a = 0$, $b \neq 0$ and for $a \neq 0$, $b = 0$; this is again due to the fact that the annihilation cross section is fixed, for given C, by the desired total Dark Matter relic density.

Recall that an increase of C beyond zero corresponds to an increase of the annihilation cross section, albeit initially a very small one (see Fig. 4). This increases the first factor in the product shown here. On the other hand, we just saw in Fig. 5 that this decreases the third factor, $Y_{\bar\chi}$. Fig. 6 shows that this second effect is always the more important one, i.e. introducing an asymmetry in the Dark Matter sector can only *reduce* the signals from Dark Matter annihilation in galactic haloes. However, this reduction is at first very mild.

[†]Electromagnetic interactions may affect the distribution of baryonic matter, which in turn can affect the Dark Matter distribution through gravitational interactions.

For constant decoupling temperature and constant cross section the product $Y_\chi \cdot Y_{\bar\chi}$ scales like $[Y_\chi(C=0)]^2 - C^2/4$, which has vanishing slope at $C = 0$. The increase of cross section required by the increase of C to keep the total Dark Matter density fixed does not change this result significantly: the positive contribution to the slope from the first factor in the product is partly canceled by the resulting decrease of the decoupling temperature, which reduces $Y_\chi(C=0)$. Recall also that initially the required cross section depends only very weakly on C.

As a result of this small negative slope at small C, the signals from WIMP annihilation in the halo still have about 20% of the strength in the symmetric case when the asymmetry C reaches 95% of its maximal value. However, beyond that point the strength of these signals plummet quickly, due to the very rapid decrease of the $\bar\chi$ relic density which we already saw earlier.

The right frame of Fig. 6 shows the normalized product of annihilation cross section, χ density and $\bar\chi$ density as function of $a + b/6$. We now observe an almost constant, negative logarithmic slope as the cross section is increased from its minimal value, which corresponds to $C = 0$. Already for small C the essentially vanishing slope in the left frame of Fig. 6 (product vs. C) combines with the very large positive slope of Fig. 4 (required C vs. cross section) to give a finite negative slope.

In particular, we find that the indirect signals from WIMP annihilation in galactic haloes are suppressed by about a factor 10^5 for a cross section about 8.2 (9.0) times the minimal allowed cross section, for $b = 0$ ($a = 0$). This opens new possibilities for model building. A suppression of the annihilation rate by a factor $\mathcal{O}(10^5)$ below the rate expected for self–conjugate thermal dark matter annihilating from an $S-$wave initial state is required if an observed excess of positrons near the galactic center [10] is to be explained [11] through the annihilation of WIMPs with masses near an MeV.[‡] In existing models [11] this is engineered by suppressing annihilation from the $S-$wave; the velocity dependence of the cross section then suppresses today's annihilation rate relative to that in the early universe. Here we see that the same suppression can be arranged for asymmetric Dark Matter, if the annihilation cross section is about one order of magnitude larger than that required for symmetric DM.

5   Summary and Conclusions

In this paper we investigated the abundance of Dark Matter for the asymmetric WIMP scenario, where Dark Matter particles and anti–particles are distinct. This opens the possibility of

---

[‡]Annihilation into e^+e^- pairs is only possible if $m_\chi > m_e$. On the other hand, astrophysical observations [12] imply $m_\chi \lesssim 10$ MeV in this case.

generating an asymmetry between WIMPs and their anti–particles. Here we assume that this happened well before the epoch of thermal decoupling of the WIMPs. We do not specify any dynamical mechanism for generating this asymmetry; rather, we treat it as a free parameter.

In our work we have assumed that the Dark Matter has reached thermal equilibrium before it decoupled. This allows a fairly generic treatment of the problem. Asymmetric Dark Matter is often motivated by explaining the origin of the baryon or lepton asymmetry. The baryogenesis or leptogenesis process is usually assumed to happen much earlier than WIMP decoupling. We note, however, that there could be cases where the WIMP density did not reach full thermal equilibrium. In that case, the abundance evolution would be model–dependent. Moreover, we assume that WIMPs can only annihilate with their anti–particles; self–annihilation of WIMPs would add additional terms to the Boltzmann equations.

The Dark Matter decoupled from the rest of the cosmic fluid, and its (co–moving) abundance froze, when the annihilation rate dropped below the Hubble expansion rate. In the asymmetric Dark Matter case, as there are more particles than anti–particles (for the reverse case, our results would be the same except that "particle" and "anti–particle" are exchanged), the anti–particles annihilated away more efficiently, with large numbers of particles left behind without partner to annihilate. As a result, the final abundance is determined not only by the cross section as in the symmetric Dark Matter case, but also by the asymmetry. We derived approximate analytical expressions for the abundance and decoupling temperature as functions of cross section and asymmetry, generalizing the well–known treatment of the (chemical) decoupling of symmetric DM.

Numerically we find that the final DM density is already largely determined by the initial asymmetry if the annihilation cross section is just two times larger than the value required for symmetric thermal DM. We also saw that introducing an asymmetry always reduces today's indirect DM detection signals from WIMP annihilation in galactic haloes: even though introducing an asymmetry requires larger annihilation cross sections to attain the desired total DM relic density, the resulting enhancement of the annihilation rate is over–compensated by the strong suppression of the final anti–WIMP density. This suppression of today's WIMP annihilation rate is desired in models where annihilation of MeV Dark Matter particles into e^+e^- pairs explains a possible excess of positrons found near the center of our galaxy.

We find that increasing the annihilation cross section by one order of magnitude suppresses today's annihilation rate by about six orders of magnitude. Today's anti–WIMP density therefore remains significant only for a rather narrow range of annihilation cross sections above the value required for symmetric dark matter.

Note Added

As we were preparing this manuscript, ref. [13] appeared, in which the problem of asymmetric WIMP Dark Matter decoupling is also investigated. While the general ideas are similar, the main focus of the paper and the details of the treatment are different. In particular, ref. [13] presents analytical expressions only for the difference and the ratio of the (co–moving) χ and $\bar{\chi}$ densities. Numerically our results are in general agreement with theirs.

Acknowledgments

References

[1] N. Jarosik *et al.*, Astrophys. J. Suppl. **192**, 14 (2011) E. Komatsu *et al.*, Astrophys. J. Suppl. **192**, 18 (2011)

[2] For a review, see G. Bertone, D. Hooper and J. Silk, Phys. Rep. **405**, 279 (2005) [hep-ph/0404175]; G. Jungman, M. Kamionkowski, and K. Griest, Phys. Rep. **267**, 195 (1996)

[3] S. Nussinov, Phys. Lett. B **165**, 55 (1985); K. Griest and D. Seckel. Nucl. Phys. B **283**, 681 (1987); R.S. Chivukula and T.P. Walker, Nucl. Phys. B **329**, 445 (1990); D.B. Kaplan, Phys. Rev. Lett. **68**, 742 (1992); D. Hooper, J. March-Russell and S.M. West, Phys. Lett. B **605**, 228 (2005) [arXiv:hep-ph/0410114]; K Belotsky, D. Fargion, M. Khlopov and R. Konoplich, Phys. Atom. Nucl. **71**, 147 (2008) [arXiv:hep-ph/0411093]; M. Yu. Khlopov, JETP Letters **83**, 1 (2006) [arXiv:astro-ph/0511796]; D. Suematsu, Astropart. Phys. **24**, 511 (2006) [arXiv:hep-ph/0510251]; M. Yu. Khlopov and C. Kouvaris, Phys. Rev. D **78** (2008) 065040 [arXiv: 0806.1191 [astro-ph]]; E. Nardi, F. Sannino and A. Strumia, JCAP **0901** (2009) 043 [arXiv:0811.4153v1 [hep-ph]]; H. An, S.L. Chen, R.N. Mohapatra and Y. Zhang, JHEP **1003**, 124 (2010) [arXiv:0911.4463 [hep-ph]]; T. Cohen and K.M. Zurek, Phys. Rev. Lett. **104**, 101301 (2010) [arXiv:0909.2035 [hep-ph]]. D.E. Kaplan, M.A. Luty

and K.M. Zurek, Phys. Rev. D **79**, 115016 (2009) [arXiv:0901.4117 [hep-ph]]; T. Cohen, D.J. Phalen, A. Pierce and K.M. Zurek, Phys. Rev. D **82**, 056001 (2010) [arXiv:1005.1655 [hep-ph]]; J. Shelton and K.M. Zurek, Phys. Rev. D **82**, 123512 (2010) [arXiv:1008.1997 [hep-ph]]; H. Davoudiasl, D.E. Morrissey, K. Sigurdson and S. Tulin, Phys. Rev. Lett. **105**, 211304 (2010) [arXiv:1008.2399 [hep-ph]]; N. Haba and S. Matsumoto, arXiv:1008.2487 [hep-ph]; M.R. Buckley and L. Randall, arXiv:1009.0270 [hep-ph]; P.-H. Gu, M. Lindner, U. Sarkar and X. Zhang, arXiv:1009.2690 [hep-ph]; M. Blennow, B. Dasgupta, E. Fernandez-Martinez and N. Rius, JHEP **1103**, 014 (2011) [arXiv:1009.3159 [hep-ph]]; L.J. Hall, J. March-Russell and S.M. West, arXiv:1010.0245 [hep-ph]; B. Dutta and J. Kumar, arXiv:1012.1341 [hep-ph]; A. Falkowski, J.T. Ruderman and T. Volansky, arXiv:1101.4936 [hep-ph]; J.J. Heckman and S.-J. Rey, arXiv:1102.5346 [hep-th]; M.T. Frandsen, S. Sarkar and K. Schmidt-Hoberg, [arXiv:1103.4350 [hep-ph]].

[4] A. Belyaev, M. T. Frandsen, F. Sannino and S. Sarkar, Phys. Rev. D **83**, 015007 (2011) [arXiv:1007.4839].

[5] R.J. Scherrer and M.S. Turner, Phys. Rev. D **33**, 1585 (1986), Erratum-ibid. D **34**, 3263 (1986); P. Gondolo and G. Gelmini, Nucl. Phys. B **360**, 145 (1991).

[6] M. Drees, M. Kakizaki and S. Kulkarni, Phys. Rev. D **80**, 043505 (2009) [arXiv:0904.3046 [hep-ph]].

[7] M. Kamionkowski and M.S. Turner, Phys. Rev. D **42**, 3310 (1990); D.J.H. Chung, E.W. Kolb and A. Riotto, Phys. Rev. D **60**, 063504 (1999) [arXiv:hep-ph/9809453]; T. Moroi and L. Randall, Nucl. Phys. B **570**, 455 (2000) [arXiv:hep-ph/9906527]; G.F. Giudice, E.W. Kolb and A. Riotto, Phys. Rev. D **64**, 023508 (2001) [arXiv:hep-ph/0005123]; R. Allahverdi and M. Drees, Phys. Rev. Lett. **89**, 091302 (2002) [arXiv:hep-ph/0203118], and Phys. Rev. D **66**, 063513 (2002) [arXiv:hep-ph/0205246]; P. Salati, Phys. Lett. B **571**, 121 (2003) [arXiv:astro-ph/0207396]; S. Profumo and P. Ullio, JCAP **0311**, 006 (2003) [arXiv:hep-ph/0309220]; C. Pallis, Astropart. Phys. **21**, 689 (2004) [arXiv:hep-ph/0402033]; R. Catena, N. Fornengo, A. Masiero, M. Pietroni and F. Rosati, Phys. Rev. D **70**, 063519 (2004) [arXiv:astro-ph/0403614]; N. Okada and O. Seto, Phys. Rev. D **70**, 083531 (2004) [arXiv:hep-ph/0407092]; A.B. Lahanas, N.E. Mavromatos and D.V. Nanopoulos, Phys. Lett. B **649**, 83 (2007) [arXiv:hep-ph/0612152].

[8] M. Drees, H. Iminniyaz and M. Kakizaki, Phys. Rev. D **73**, 123502 (2006) [arXiv:hep-ph/0603165], and Phys. Rev. D **76**, 103524 (2007) [arXiv:0704.1590 [hep-ph]].

[9] K. Griest and D. Seckel, Phys. Rev. D **43** (1991) 3191.

[10] P. Jean et al., Astron. Astrophys. **407** L55 (2003) [arXiv: astro-ph/0309484].

[11] C. Boehm, D. Hooper, J. Silk, M. Casse and J. Paul, Phys. Rev. Lett. **92** 101301 (2004), [arXiv: astro-ph/0309686].

[12] J.F. Beacom, N.F. Bell and G. Bertone, Phys. Rev. Lett. **94** 171301 (2005) [astro-ph/0409403]; L. Zhang, X.-L. Chen, Y.-A. Lei and Z.-G. Si, Phys. Rev. D **74** 103519 (2006) [astro-ph/0603425]; M. Valdes, A. Ferrara, M. Mapelli and E. Ripamonti, Mon. Not. Roy. Astron. Soc. **377** 245 (2007) [astro-ph/0701301]; A. Natarajan and D. J. Schwarz, Phys. Rev. D **78** 103524 (2008) [arXiv:0805.3945 [astro-ph]].

[13] M. L. Graesser, I. M. Shoemaker and L. Vecchi, [arXiv:1103.2771 [hep-ph]].